Available online at www.sciencedirect.com
ScienceDirect
Journal of Nuclear Materials 363–365 (2007) 844–848
journal of nuclear materials
www.elsevier.com/locate/jnucmat

Thermal interaction of plasma with Gas Puffing

P. Tamain *, E. Tsitrone, Ph. Ghendrih, J. Gunn, F. Clairet, J. Bucalossi, B. Pégourié

Association EURATOM-CEA, CEA Cadarache, F-13108 St. Paul-lez-Durance, France

Abstract

This paper presents a model of gas injection treating coherently matter deposition and thermal effects on the plasma. It is demonstrated from an analytical model that an injection can trigger thermal bifurcations toward radiative or recombinant regimes. 1D simulations were performed to study the radial dynamics. They indicate that the injection can create a cold detached region in the outer plasma. The ionization front is located at the transition between this zone and the hot plasma, characterized by a radiative layer and strong temperature gradients. In spite of a better neutral penetration, strong sources are needed for efficient core fuelling and extrapolations for ITER remain pessimistic. Moreover a thermal instability linked to the bifurcation is evidenced for strong particle sources. However, a 1D parallel model shows that the perturbation linked to the injection can remain localized along the parallel direction, thus favoring neutrals penetration, but this effect strongly depends on the perpendicular–parallel transport interplay.

PACS: 52.25.Ya; 52.30.−q; 52.30.Ex; 52.65.−y

1. Introduction

Plasma fuelling is a major issue for future tokamaks since it is a fundamental parameter for building high performance profiles. In ITER, a fuel ions flux to the core of 2 Pa m^3 s^{-1} will be required in steady state [1]. These particles will have to penetrate through the pedestal ($T_e \approx 3$–5 keV at the top) without affecting the H-mode confinement.

The fuelling methods foreseen for ITER are Gas Puffing (GP) [2] and Pellet Injection (PI) [3]. GP is a simple method but fuelling efficiency is limited (∼10% on Tore-Supra (TS)) and neutral penetration length suggests a negligible core fuelling in ITER (<1% of injected particles). PI presents much better fuelling efficiencies (∼90% on TS), but it will still provide only shallow fuelling for ITER and its practical implementation remains an issue. An alternative method, Supersonic Molecular Beam Injection (SMBI), has been tested in TS and has demonstrated an improved fuelling efficiency (∼50%) compared to GP, while using a simpler technology than PI [4]. This improved efficiency has been attributed to the strong thermal interaction of the injection neutrals with the plasma and its impact on neutrals penetration length and parallel losses to the wall.

* Corresponding author. Tel.: +33 44225 7693.
E-mail address: patrick.tamain@cea.fr (P. Tamain).

0022-3115/$ - see front matter
doi:10.1016/j.jnucmat.2007.01.235

However, no coherent modelling of this phenomenon has been performed yet [5], whereas taking these effects into account might change extrapolations for ITER.

This paper describes a model of GP and its interaction with the edge plasma including thermal effects coherently. Section 2 presents an analytical 2-reservoir model which demonstrates that a strong particle injection can trigger thermal bifurcations. In Section 3, we use 1D radial simulations to investigate the issues of neutrals penetration and radial dynamics. The question of the parallel localization of the perturbation is addressed in Section 4.

2. Analytical study of injection-triggered thermal bifurcations

2.1. Electronic temperature dependencies

The key point of the forthcoming models lies on the dependence of atomic processes with electronic temperature. Fits for ionization rate $\langle\sigma v\rangle_{\mathrm{i}}$, recombination rate $\langle\sigma v\rangle_{\mathrm{rec}}$, ionization energy loss per ionization event E_{i} and radiative loss function L_Z were taken from Ref. [6]. They are displayed in Fig. 1. Main features that should be noticed are the sharp peak of L_Z whose position, T_{rad}, depends on the considered radiating specie, the collapse of the ionization rate for $T_{\mathrm{e}} \lesssim 2$–3 eV and the rise of E_{i} at low temperatures while being nearly constant for $T_{\mathrm{e}} > 10$ eV.

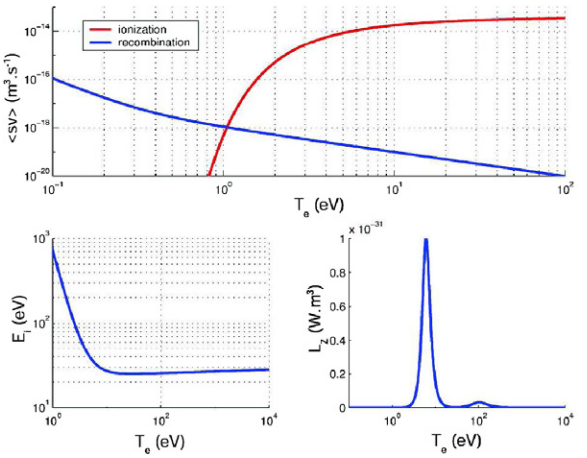

Fig. 1. Electronic temperature dependencies of ionization rate $\langle\sigma v\rangle_{\mathrm{i}}$, recombination rate $\langle\sigma v\rangle_{\mathrm{rec}}$, ionization energy per ionization event E_{i} and radiative loss function L_Z.

2.2. 0D model for thermal bifurcations

The plasma is described in limiter configuration and divided into two homogeneous layers separated by the Last Closed Magnetic Surface (LCFS): the Scrape Off Layer (SOL) and the Core (C). Matter and energy balances in both layers are derived according to the flux pattern given in Fig. 2 with a given energy source P_{add} in the core and particle source S at the outer wall, as well as a given proportion C_Z of radiating impurities. The parallel sink to the limiter includes both convective and conductive losses. Three neutral species are considered: neutrals injected from the wall with a given inward velocity, neutrals recycling from the limiter into the core and recombination neutrals which stay in the layer where they are born. The temperature of the core is assumed to be high enough so as not to consider radiation losses nor recombination in this layer (see Section 2.1). For the same reason, the ionization energy E_{i} and reaction rate $\langle\sigma v\rangle_{\mathrm{i}}$ are considered as constant in the core. $T_{\mathrm{e}} = T_{\mathrm{i}} = T$ is assumed.

Combining balance equations in each layer leads to the total energy balance as a function of the temperature in the SOL, T_{SOL}, only. This equation takes the following form:

$$P_{\mathrm{add}} = f_{\mathrm{losses}}(T_{\mathrm{SOL}}, S, \ldots), \tag{1}$$

where f_{losses} is the total power loss function. It is then straightforward to solve the equilibrium to obtain T_{SOL} as a function of P_{add} and S.

Fig. 3 shows the shape of f_{losses} with respect to T_{SOL}. A S shaped curve typical of thermal bifurcations [7] is found. Three different branches can be distinguished: an attached branch at high temperature, a radiative branch at temperatures $T_{\mathrm{SOL}} \lesssim T_{\mathrm{rad}}$ ($\sim$5 eV in Fig. 3's case with carbon) and a recombinant branch at low temperatures ($T_{\mathrm{SOL}} \lesssim 1$ eV) linked to the drop of the ionization rate. Particle sources with high injection rates (SMBI,

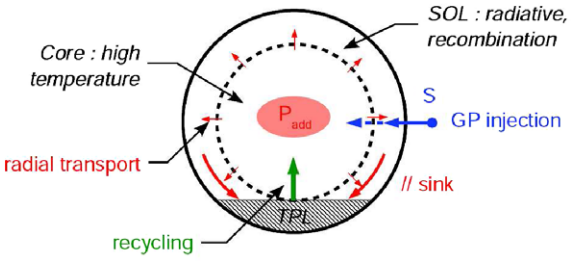

Fig. 2. Matter and energy fluxes treated in the analytical model.

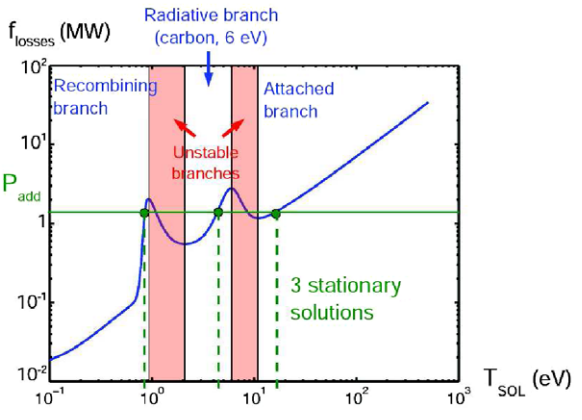

Fig. 3. Energy loss function as a function of the SOL temperature T_{SOL} for a typical TS case with $C_Z = 0.05$ of carbon and $S = 5\times10^{21}\ \mathrm{s}^{-1}$.

for example) are in the typical range to reach a recombinant solution.

3. Radial dynamics modelling

3.1. Model equations

To investigate the influence of thermal bifurcations on matter deposition and plasma stability, consider a radial model of GP based on the following equations:

$$n_{\mathrm{e}} = n_{\mathrm{i}} + Z_{\mathrm{imp}} n_{\mathrm{imp}}, \tag{2}$$

$$\begin{aligned}\partial_t n_{\mathrm{i}} = {} & \partial_{\mathrm{r}}(D_\perp \partial_{\mathrm{r}} n_{\mathrm{i}} - v_{\mathrm{pinch}} n_{\mathrm{i}}) - \langle\sigma v\rangle_{\mathrm{rec}} n_{\mathrm{e}} n_{\mathrm{i}} \\ & + \langle\sigma v\rangle_{\mathrm{i}} n_{\mathrm{e}} (n_{\mathrm{n}} + n_{\mathrm{nS}} + n_{\mathrm{nR}}) \\ & - \delta_{r\in\mathrm{SOL}} \frac{n c_{\mathrm{s}}}{2\pi r} \sin\alpha_{\mathrm{inc}},\end{aligned} \tag{3}$$

$$\partial_t n_{\mathrm{n}} = \partial_{\mathrm{r}}(D_{\perp\mathrm{n}} \partial_{\mathrm{r}} n_{\mathrm{n}}) + \langle\sigma v\rangle_{\mathrm{rec}} n_{\mathrm{e}} n_{\mathrm{i}} - \langle\sigma v\rangle_{\mathrm{i}} n_{\mathrm{e}} n_{\mathrm{n}}, \tag{4}$$

$$v_{\mathrm{inj}} \partial_{\mathrm{r}} n_{\mathrm{nS}} = \langle\sigma v\rangle_{\mathrm{i}} n_{\mathrm{e}} n_{\mathrm{nS}}, \tag{5}$$

$$\begin{aligned}v_{\mathrm{recycl}} \partial_{\mathrm{r}} n_{\mathrm{nR}} = {} & \langle\sigma v\rangle_{\mathrm{i}} n_{\mathrm{e}} n_{\mathrm{nR}} \\ & - \delta_{r\in\mathrm{SOL}} P_{\mathrm{recycl}} \frac{n c_{\mathrm{s}}}{2\pi r} \sin\alpha_{\mathrm{inc}},\end{aligned} \tag{6}$$

$$\begin{aligned}\frac{3}{2} n_{\mathrm{e}} \partial_t T_{\mathrm{e}} = {} & \partial_{\mathrm{r}}\left(K^{\mathrm{e}}_\perp \partial_{\mathrm{r}} T_{\mathrm{e}} - \frac{3}{2} v_{\mathrm{pinch}} n_{\mathrm{e}} T_{\mathrm{e}}\right) \\ & - \langle\sigma v\rangle_{\mathrm{i}} n_{\mathrm{e}} (n_{\mathrm{n}} + n_{\mathrm{nS}} + n_{\mathrm{nR}}) E_{\mathrm{i}} \\ & - \frac{3}{2} \langle\sigma v\rangle_{\mathrm{rec}} n_{\mathrm{e}} n_{\mathrm{i}} T_{\mathrm{e}} - L_Z n_{\mathrm{e}} n_{\mathrm{imp}} - \alpha(T_{\mathrm{e}} - T_{\mathrm{i}}) \\ & - \delta_{r\in\mathrm{SOL}} \frac{\gamma_{\mathrm{e}} n_{\mathrm{e}} c_{\mathrm{s}} T_{\mathrm{e}}}{2\pi r} \sin\alpha_{\mathrm{inc}},\end{aligned} \tag{7}$$

$$\begin{aligned}\frac{3}{2} n_{\mathrm{i}} \partial_t T_{\mathrm{i}} = {} & \partial_{\mathrm{r}}\left(K^{\mathrm{i}}_\perp \partial_{\mathrm{r}} T_{\mathrm{i}} - \frac{3}{2} v_{\mathrm{pinch}} n_{\mathrm{i}} T_{\mathrm{i}}\right) - \frac{3}{2} \langle\sigma v\rangle_{\mathrm{rec}} n_{\mathrm{e}} n_{\mathrm{i}} T_{\mathrm{i}} \\ & + \alpha(T_{\mathrm{e}} - T_{\mathrm{i}}) - \delta_{r\in\mathrm{SOL}} \frac{\gamma_{\mathrm{i}} n_{\mathrm{i}} c_{\mathrm{s}} T_{\mathrm{i}}}{2\pi r} \sin\alpha_{\mathrm{inc}}.\end{aligned} \tag{8}$$

A given density n_{imp} of impurities of charge Z_{imp} is considered. Balance equations for ions, neutrals, electronic temperature and ionic temperature (Eqs. (3)–(8)) are treated. Three neutral species are considered and handled in a fluid description: injected neutrals (density n_{nS}) with given inward speed v_{inj}, neutrals which recycle toward the center at velocity v_{recycl} (density n_{nR}), and recombination neutrals (density n_{n}) whose transport is described through a diffusion coefficient $D_{\perp\mathrm{n}}$. The two formers are assumed to be in steady state since their fly time across the simulation box is lower than the source time width: $\frac{a}{v_{\mathrm{inj/recycl}}} \ll \tau_{\mathrm{inj}}$. Perpendicular transport is described in terms of anomalous diffusion $D_\perp$ and heat diffusivity $K^{\mathrm{i/e}}_\perp$, a constant pinch velocity v_{pinch} being added to perpendicular fluxes. All the following results have been obtained for $D_\perp = 1\ \mathrm{m}^2\ \mathrm{s}^{-1}$, $v_{\mathrm{pinch}} = -0.5\ \mathrm{m\ s}^{-1}$ and $K^{\mathrm{i/e}}_\perp = K^{\mathrm{i/e}}_{\perp 0} n_{\mathrm{i/e}}$ with $K^{\mathrm{i}}_{\perp 0} = 0.2\ \mathrm{m}^2\ \mathrm{s}^{-1}$ and $K^{\mathrm{e}}_{\perp 0} = 2\ \mathrm{m}^2\ \mathrm{s}^{-1}$, so as to work with typical TS equilibrium profiles. The parallel direction appears through a sink term in the SOL which includes both convective and conductive transport. Electronic and ionic temperatures are distinguished, radiation (L_Z) and ionization (E_{i}) losses being included in electronic energy balance. The main boundary conditions are a given incoming power flux from the core P_{add} and injection neutral density at the wall linked to the source amplitude S. The terms in $\sin\alpha_{\mathrm{inc}}$ represent the parallel sink in the SOL, α_{inc} being the incidence angle of magnetic field line on the limiter: $\sin\alpha_{\mathrm{inc}} \simeq \frac{\sqrt{r^2-a^2}}{qR}$.

3.2. Radial dynamics of plasma–GP interaction

Several simulations were performed for various values of S and P_{add}. Fig. 4 shows a result obtained for a typical SMBI on Tore-Supra with $S = 2\times10^{23}\ \mathrm{s}^{-1}$ and $P_{\mathrm{add}} = 2\ \mathrm{MW}$. As expected from the previous analysis, the injection triggers a thermal bifurcation in the outer plasma, a cold front propagating toward the center and allowing neutrals to penetrate deeper. The transition layer between the cold outer zone and the hot plasma is characterized by steep temperature gradients linked to the strong radiative power losses around $T_{\mathrm{e}} = T_{\mathrm{rad}}$ and by a sharply peaked matter deposition.

If we compare to the previous studies on SMBI [5] which did not include radiative losses, the existence of thermal bifurcations modifies the radial dynamics during an injection. It first allows better neutrals penetration for a given source amplitude.

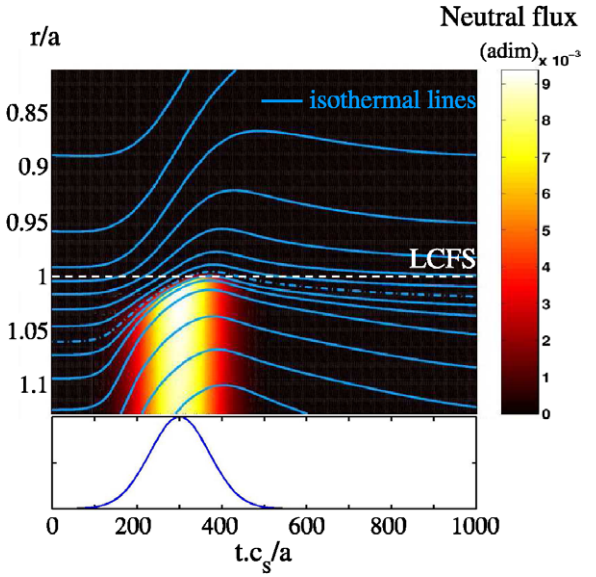

Fig. 4. Injected neutrals flux during an injection as a function of normalized time and radius. The amplitude of the source is given underneath. Isothermal lines are displayed, particularly the $T_e = T_{rad}$ one (dash-dot).

It also leads to longer relaxation times to equilibrium for the temperature profiles, which is closer to experimental results (for typical Tore-Supra cases, 0.1–0.2 s). Furthermore, the existence of a threshold on the magnitude of the source has been found over which the cold front continues to propagate inward even after the injection. This instability is evidenced in Fig. 5 where one can notice a change of behaviour in the penetration depth of the radiative front. A rough extrapolation to ITER's case ($P_{add} \simeq 100$ MW, $S \simeq 1 \times 10^{23}$ s^{-1}) is

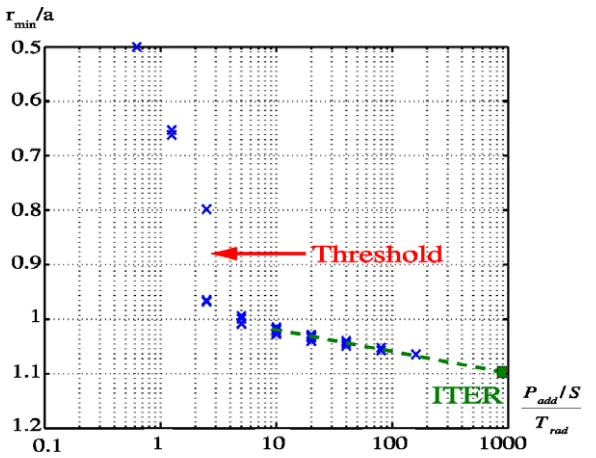

Fig. 5. Minimum radius reached by the cold front as a function of the ratio $\frac{P_{add}/S}{T_{rad}}$ and linear extrapolation for ITER's case.

also plotted. It shows a very poor penetration depth of GP neutrals, which confirms previous pessimistic estimations on GP capability to fuel ITER [8] in spite of the existence of thermal bifurcations.

4. Parallel localization of the perturbation

The latter conclusion could however be modified if the perturbation linked to the GP injection remains localized along the parallel direction: better penetration depths could be obtained with reasonnable source amplitudes without perturbing globally the plasma temperature profiles. We have addressed this issue using a 1D parallel model based on the parallel version of Eqs. (2)–(8). Density transport is convective along the parallel direction so the system is completed with the parallel momentum balance equation:

$$\partial_t \Gamma = -\partial_z \left(n(T_e + T_i) + \frac{\Gamma^2}{n} \right) + \partial_z \left(\eta \partial_z \frac{\Gamma}{n} \right), \qquad (9)$$

where Γ is the parallel ion flux. For energy transport, convective and diffusive terms are considered, Spitzer–Harm thermal conductivity being used: $K_\parallel^{e/i} = K_{\parallel 0}^{e/i} T_{e/i}^{5/2}$. Energy supply by radial transport appears as a linear source under the hypothesis that the considered field line exchanges matter and en-

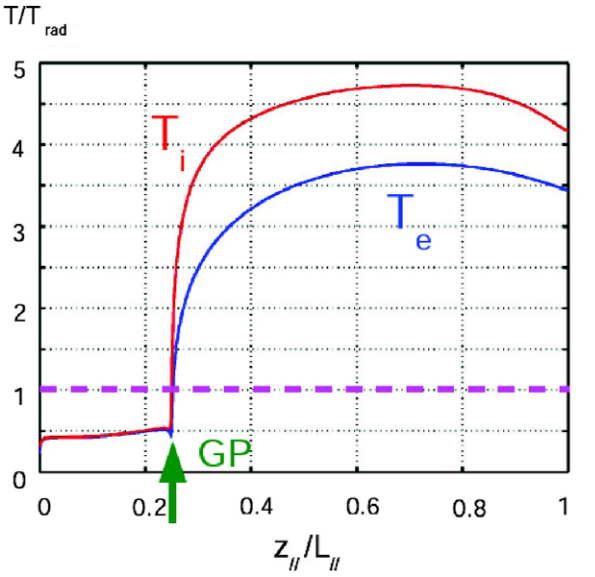

Fig. 6. Parallel profile of electronic temperature T_e (blue) and ionic temperature T_i (red) during a GP injection located at $\frac{z}{L_\parallel} = 0.25$ (equatorial plane). (For interpretation of the references in colour in this figure legend, the reader is referred to the web version of this article.)

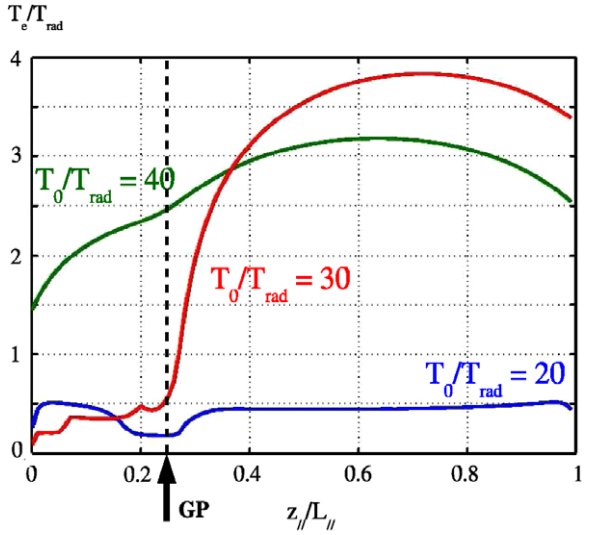

Fig. 7. Different behaviours for parallel localization of the thermal perturbation linked to the injection for three values of T_0.

ergy with another field line which is not perturbed by the injection. Source terms are then described as exchanges with a perfect matter and energy reservoir characterized by constant density n_0 and temperature T_0: $S = n_0 - n$, $S_T = T_0 - T$.

Fig. 6 shows parallel temperature profiles obtained during neutral injections. The injection point is localized in the equatorial plane at $\frac{z}{L_\parallel} = 0.25$. A thermal bifurcation can be noticed that remains localized in spite of the very strong parallel transport. The strong gradient appearing at the transition between the bifurcated region and the other side of the SOL can be sustained thanks to the dependence of $K_\parallel$ in $T^{5/2}$ as well as the presence of the radiation layer in this zone.

However, the parallel localization of the temperature collapse is closely dependent on the linear sources. This sensitive behaviour is illustrated in Fig. 7. For low values of the perpendicular transport contribution, the perturbation concerns the whole SOL while for higher values, even strong sources could not lead to any bifurcation. Thus, the interplay between parallel and perpendicular transport plays a fundamental role in the dynamics of the injection through its influence on the localization of thermal bifurcations.

5. Summary

We have investigated the interaction between the plasma and particle injection taking into account the thermal aspects coherently. The existence of thermal bifurcations has been established and we have shown that they determine the radial dynamics of matter deposition and plasma profiles during an injection and the following plasma relaxation. A significant penetration depth can be reached for high injection rates, but a thermal instability occurs for strong sources. All the same, taking into account thermal bifurcations in the 1D radial model does not change much pessimistic estimations for ITER. However, 1D parallel simulations indicate that the thermal perturbation linked to the injection can remain localized along the field lines. Such an effect is promising for neutral penetration, but simulations exhibit a strong dependence on the perpendicular–parallel transport interplay. This result shall be investigated in further studies.

References

[1] ITER Teams, Nucl. Fusion 39 (1999) 2391.
[2] C.S. Pitcher, Vac. Technol. Appl. Ion Phys. 38 (1988) 1059.
[3] S.L. Milora et al., Nucl. Fusion 35 (1995) 657.
[4] J. Bucalossi, et al., in: Proceedings of 19th IAEA Fusion Energy Conferences, Lyon, October 2002, EX/P4-04.
[5] B. Pégourié et al., J. Nucl. Mater. 313–316 (2003) 539.
[6] P.C. Stangeby, The Plasma Boundary of Magnetic Fusion Devices, IoP, 2000, p. 111.
[7] H. Capes, Ph. Ghendrih, A. Samain, Phys. Fluids 4 (1992) 1287.
[8] G. Federici et al., J. Nucl. Mater. 313–316 (2003) 11.